NL
=
Delong

AFRL-SR-AR-TR-06-0328

REPORT DOCUMENTATION PAGE

The public reporting burden for this collection of information is estimated to average 1 hour per response, including the time gathering and maintaining the data needed, and completing and reviewing the collection of information. Send comments regarding information, including suggestions for reducing the burden, to the Department of Defense, Executive Services and Communica that notwithstanding any other provision of law, no person shall be subject to any penalty for failing to comply with a collect control number.
PLEASE DO NOT RETURN YOUR FORM TO THE ABOVE ORGANIZATION.

1. REPORT DATE *(DD-MM-YYYY)* 30-06-2006	2. REPORT TYPE Final Technical	3. DATES COVERED *(From - To)* 01-05-2005 - 31-03-2006

4. TITLE AND SUBTITLE Integrated Nanoscale Nanowire Correlated Electronic Nanosensing Technology (INNOCENT)	5a. CONTRACT NUMBER
	5b. GRANT NUMBER FA9550-05-1-0279
	5c. PROGRAM ELEMENT NUMBER
6. AUTHOR(S) Charles M. Lieber	5d. PROJECT NUMBER
	5e. TASK NUMBER
	5f. WORK UNIT NUMBER

7. PERFORMING ORGANIZATION NAME(S) AND ADDRESS(ES) President and Fellows of Harvard College, Office for Sponsored Programs 1350 Massachusetts Avenue Cambridge, MA 02138	8. PERFORMING ORGANIZATION REPORT NUMBER

9. SPONSORING/MONITORING AGENCY NAME(S) AND ADDRESS(ES) Air Force Office for Scientific Research 875 North Randolph St. Suite 325, Room 3112 Arlington, VA 22203	10. SPONSOR/MONITOR'S ACRONYM(S)
	11. SPONSOR/MONITOR'S REPORT NUMBER(S)

Dr. Hugh Delong / NL

12. DISTRIBUTION/AVAILABILITY STATEMENT
Approved for Public Release; distribution is unlimit

20060804051

13. SUPPLEMENTARY NOTES

14. ABSTRACT
Development of highly-integrated, ultra-sensitive real-time electronic sensor arrays for detection of chemical&biological threats has been carried out by exploiting the unique electronic properties and integration potential of nanowire electronic devices. Silicon nanowires have been developed and assembled into arrays of sensor elements that provide highly-robust and specific ultra-sensitive species identification while at the same time dramatically reducing false positives. Sensor modalities developed in this project is based on nanowire field-effect transistors, where unique specificities of sensor elements for chemical&biological threats has been achieved through specific surface modification using designed chemical and biological receptors for threats of interest. Experiments have demonstrated biothreat (viruses&toxins) detection at better than 1 picomolar sensitivity, detection chemical (explosive) threats at better than 100 parts per billion sensitivity, simultaneous multiplexed detection from ten or more addressable nanowire sensing elements, and moreover, signal processing algorithms that allow for discrimination of real/false signals in presence of noise were developed.

15. SUBJECT TERMS
nanowires, field-effect sensors, real-time detection, ultrasensitive detection, biological agents, viruses, proteins, toxins, chemical agents, explosives

16. SECURITY CLASSIFICATION OF:			17. LIMITATION OF ABSTRACT	18. NUMBER OF PAGES	19a. NAME OF RESPONSIBLE PERSON Webb Brightwell
a. REPORT	b. ABSTRACT	c. THIS PAGE		27	19b. TELEPHONE NUMBER *(Include area code)* 617-384-7673

Standard Form 298 (Rev. 8/98)
Prescribed by ANSI Std. Z39.18

Final Technical Report for
GRANT NUMBER FA9550-05-1-0279
1 May 2005 – 31 March 2006

Table of Contents

II TECHNICAL REPORT

A. Executive Summary

Highly-integrated, ultra-sensitive real-time electronic detection of chemical and biological threats represent a significant challenge to the current frontiers of research in biology, chemistry and engineering that could be met by exploiting the unique electronic properties and integration potential of molecular electronic devices. The challenges inherent in building highly-integrated real-time electronic nanosensing devices are great, but recent breakthroughs in nanowire growth, surface functionalization and device properties, coupled to large-scale assembly into defect and fault tolerant arrays have begun to show that aggressive program goals can be met and even exceeded in important new directions with our approach.

We have and continue to develop and assemble into arrays of powerful and distinct types of sensor elements that provide highly-robust and specific ultra-sensitive species identification while at the same time dramatically reducing false positives. The sensor modalities that we have demonstrated to date include nanowire field-effect transistor and piezoelectric nanowire resonator devices. Each of these classes of sensor devices has either demonstrated or has the potential to be designed with sensitivities that have the potential to exceed the program end goals. During the base period of the MoleSensing program we have met the Program milestones and demonstrated the great potential of our approach. A summary of results achieved to data are as follows:

- **Demonstrated detection of biomolecules at $\leq 1\times 10\text{-}12$ M**
  - demonstrated reversible detection of proteins and viruses at $\leq 10\text{-}12$ M
  - demonstrated concentration-dependent detection over ≥ 104 range
  - demonstrated high-selectivity, including complex mixtures
- **Demonstrated detection of chem-threats at 100ppb or better**
  - demonstrated detection of chem threats at ≤ 100ppb
  - demonstrated concentration-dependent detection over ≥ 103 range
  - demonstrated high-selectivity
- **Demonstrated receptor personalization & multiplexing**
  - demonstrated nanowire-receptor array platform for multiplexing
  - demonstrated simultaneous detection from > 10 elements
  - demonstrated methods for false positive discrimination
- **Demonstrated analysis for real/false signal discrimination**
  - demonstrated analysis of raw data using boolean detection (yes or no) that is robust to all expected noise sources and contamination

Continuation of this MoleSensing effort promises to lead to revolutionary advances in integrated, ultra-sensitive electronic chem/bio sensor arrays that should drive leading-edge Battle-Field and National Security defense applications.

B. SCIENTIFIC RESULTS

A summary of the results and achievements of our effort during the first base period of the program, which address successfully the program milestones, are described below.

1. Ultrasensitive protein/toxin detection. The conversion of silicon nanowire field-effect transistors into sensors for protein/toxin detection was carried out by attaching monoclonal antibodies to the nanowire surfaces following device fabrication. The basic linkage chemistry is similar to that used previously for protein microarrays, and involves three key steps. First, aldehyde propyltrimethoxysilane (APTMS) is coupled to oxygen plasma-cleaned silicon nanowire surfaces in order to present terminal aldehyde groups at the nanowire surface. Second, the aldehyde groups are coupled to the monoclonal antibodies, and third unreacted free aldehyde groups are blocked by reaction with ethanolamine.

The basic nanowire sensor chip consists of integrated electrically addressable silicon nanowires with the potential for ca. 200 individually addressable devices. A key feature of our basic array design is that it enables incorporation of different types of addressable nanowires, for example p-type and n-type doped silicon nanowires, during fabrication steps to form the addressable electrical contacts. In addition, different receptors can be printed on the nanowire device array to enable selective multiplexed detection.

The sensitivity limits of these silicon nanowire devices for protein detection were first determined by measuring conductance changes as the solution concentration of PSA was varied, where the devices were modified with monoclonal antibodies for PSA (Ab1). Representative time-dependent data show a well-defined conductance increase and subsequent return to baseline when PSA solution and pure buffer, respectively, are alternately delivered through a microfluidic channel to the devices. A plot of these data shows that the conductance
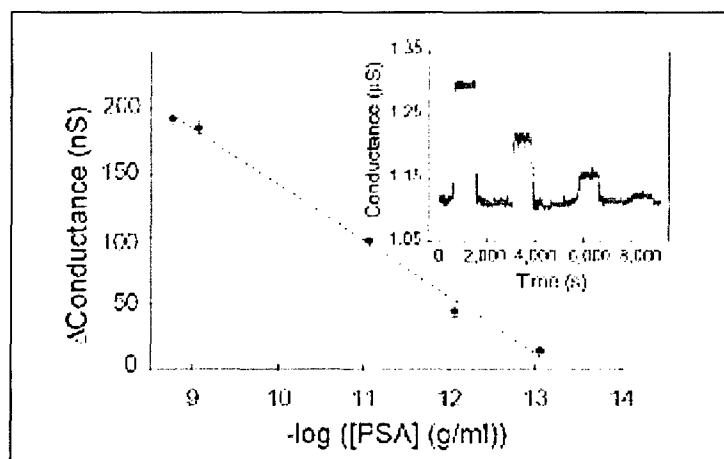

change is directly proportional to the solution PSA concentration for values from ca. 5 ng/mL down to 90 fg/mL. These data show that direct label-free detection of PSA is routinely achieved with signal to noise >3 for concentrations down to 75 fg/ml or ca. 2 fM. Significantly, similar ultrasensitive detection was achieved in studies of carcinoembryonic antigen (CEA), 100 fg/ml or 0.55 fM, and mucin-1, 75 fg/ml or 0.49 fM, using silicon nanowire devices modified with monoclonal antibodies for CEA and mucin-1, respectively.

The reproducibility and selectivity of the nanowire devices was further investigated in competitive binding experiments with bovine serum albumin (BSA). Conductance versus time measurements recorded on a silicon nanowire device modified with Ab1 exhibited

4

similar conductance changes as above when 9 and 0.9 pg/ml solutions of PSA were delivered to the device. These results show that reproducible device to device sensitivity is achieved with these silicon nanowire sensors. Moreover, delivery of a solution containing 0.9 pg/ml PSA and 10 □g/ml BSA showed the same conductance increase as a solution containing only PSA at this concentration, while no conductance change was observed in the device when the BSA solution alone was delivered. These latter data demonstrate excellent selectivity using the antibody receptors and also that our high sensitivity is not lost even with 10-million fold higher concentration of other proteins in solution.

False positive discrimination using multiple nanowire elements. We also characterized nanowire device arrays containing both p-type and n-type silicon nanowire devices that were modified with Ab1 as the marker protein receptor. The incorporation of p- and n-type nanowires in a single sensor chip enables possible electrical cross-talk and/or false positive signals to be discriminated by correlating the response versus time from the two distinct types of device elements. Notably, simultaneous conductance versus time data recorded from p-type nanowire (NW1) and n-type nanowire (NW2) devices showed that introduction of 0.9 ng/ml of PSA results in a conductance increase in NW1 and a conductance decrease in NW2, while the conductance returned to the baseline value of each device following introduction of buffer
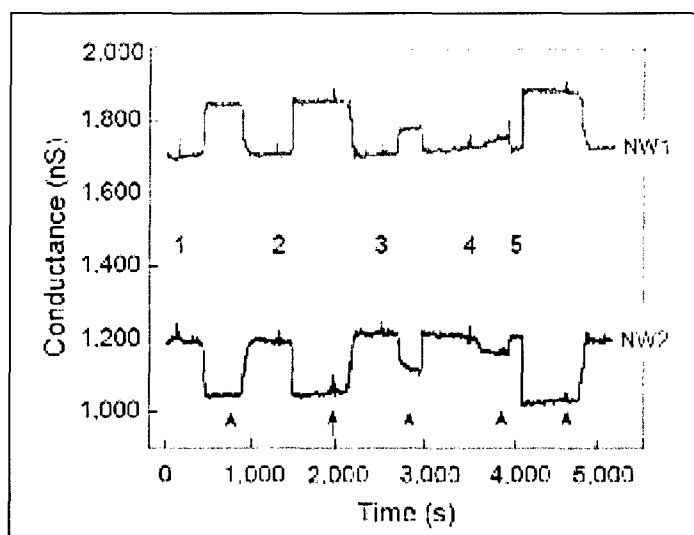
solution without PSA. These experiments demonstrate key points about multiplexed electrical detection with nanowire devices. First, the complementary conductance changes observed for the p-type and n-type elements are consistent with specific binding of PSA to field-effect devices, since the negatively-charged protein will cause accumulation and depletion in the p- and n-type nanowire elements, respectively. Second, the complementary electrical signals from p- and n-type devices provide simple yet robust means for detecting false positive signals from either electrical noise or nonspecific binding of protein to one device; that is, real and selective binding events must show complementary responses in the p- and n-type devices. The presence of correlated conductance signals in both devices, which occur at points when buffer and PSA/buffer solutions are changed, illustrate clearly how this multiplexing capability can be used to distinguish unambiguously noise from protein binding signals.

In addition, a second test of using arrays to discriminate against false positives was carried out using a device array consisting of p-type silicon nanowire elements with either PSA Ab1 receptors (NW1) or surfaces passivated with ethanolamine (NW2).

5

Simultaneous measurements of the conductance of NW1 and NW2 show that well-defined concentration-dependent conductance increases are only observed in NW1 upon delivery of PSA solutions (9 and 1 pg/ml), although small conductance spikes are observed in both devices at the points where PSA and buffer solutions are changed. Delivery of BSA at 10 □g/ml showed no response in either NW1 or NW2, and subsequent delivery of a solution of PSA (1 ng/ml) and Ab1 (1□g/ml), which complexes the free PSA, did not exhibit measurable conductance changes in either device. Together, these experiments
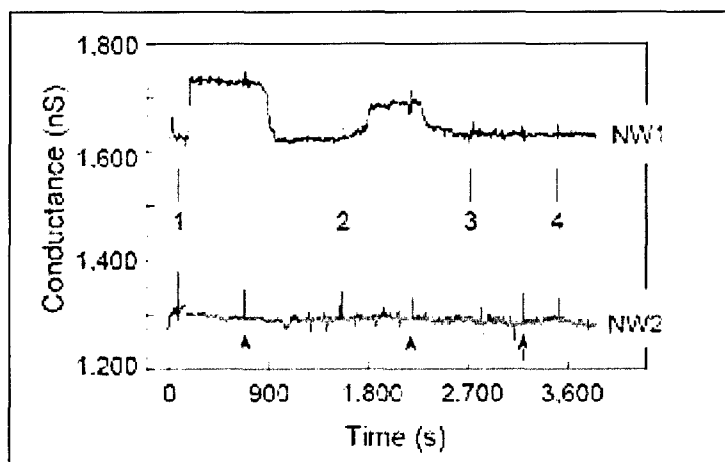

demonstrate that the electronic signals measured in the nanowire arrays can be readily attributed to selective protein binding, show that our surface chemistry effectively prevents nonspecific protein binding, and also provide a robust means for discriminating against false positive signals arising from either electronic noise or nonspecific binding.

2. Detection of single viruses. We have used arrays of individually addressable silicon nanowire FETs, which were functionalized with the same or different virus-specific antibodies as receptors, to characterize the virus detection limits. Time-dependent conductance data recorded simultaneously from two nanowires in the same device array modified with antibodies specific for influenza A virus showed discrete changes in conductance when a solution containing ca. 100 virus particles/□L is delivered to the sensor elements. There are several key features of these experiments. First, the magnitude and

6
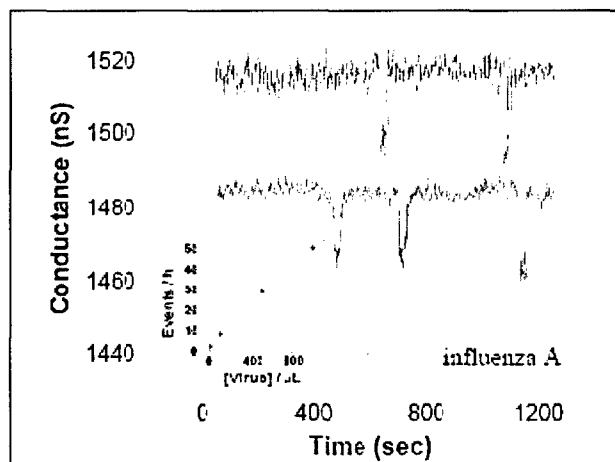
duration of the conductance drops are nearly the same for a given nanowire: for nanowires 1 and 2 the magnitude and duration are 24 ± 1 nS and 20 ± 4 s, and 20 ± 3 nS and 15 ± 7 s, respectively. The similarity in responses is consistent with good reproducibility in the nanowires electronic properties and a uniform density of antibody receptors on their surfaces, which determine the response to and duration of binding of a single virus, respectively. Second, an excess of free antibody added to the viral solution (monoclonal anti-hemagglutinin for influenza A was added to a standard solution containing 100 virons/□L to yield a antibody concentration of 10 □g/ml) eliminates the well-defined conductance changes consistent with blocking sites on the viruses that are recognized by the same antibodies attached to the nanowire surfaces. Lower antibody concentrations produced partial reduction of the nanowire response. Third, the discrete conductance changes are uncorrelated for the two nanowire devices in the microfluidic channel, and are thus consistent with stochastic binding events at or near the surfaces of the respective nanowires. Lastly, little or no purification of virus samples is required in these measurements; that is, similar results were obtained on samples purified by simple gel filtration or diluted directly from allantoic fluid.

To characterize the discrete conductance changes further, we have carried out simultaneous electrical and optical measurements. Parallel collection of conductance, fluorescence and bright-field data from a single nanowire device using fluorescently-labeled viruses demonstrate clearly that each discrete conductance change corresponds to a single virus binding to and unbinding from the nanowire.
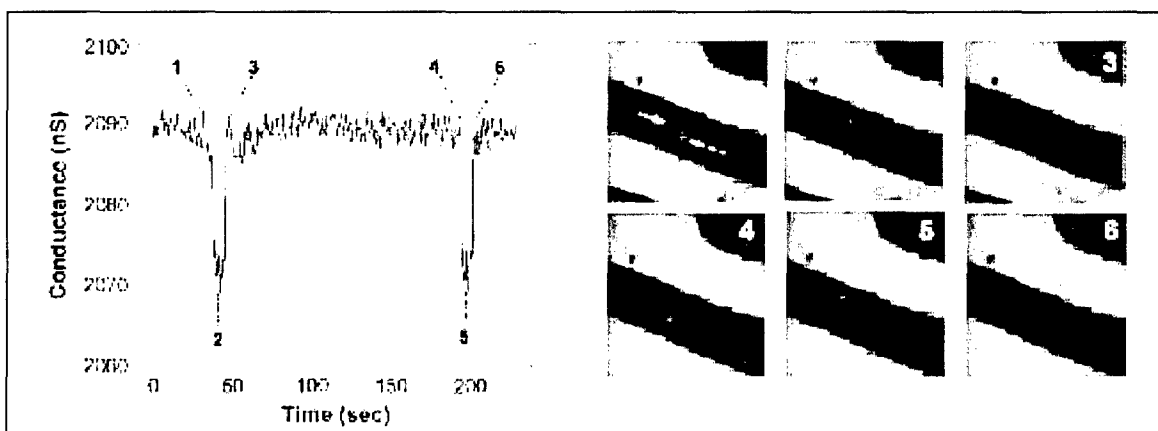
The data show that as a virus particle diffuses near a nanowire device the conductance remains at the baseline value, and only after binding at the nanowire surface does the conductance drop, where the conductance change, 18 ± 1 nS, is similar to that observed with unlabeled viruses; as the virus unbinds and diffuses from the nanowire surface the conductance returns rapidly to the baseline value. The movie further shows that a bound virus can sample several nearby positions on the nanowire surface prior to unbinding, and this may explain the smaller variations in conductance in the on state. The two events also exhibit similar conductance changes when virus particles bind to distinct sites on the nanowire, and thus demonstrate that the detection sensitivity is relatively uniform along the length of the nanowire. Lastly, these parallel measurements indicate that a virus particle must be in contact with the nanowire device to yield an electrical response, thus suggesting the potential for relatively dense integration without crosstalk.

Selective detection—the ability to specifically distinguish one type of virus from another—is crucial for exploiting the high sensitivity of these nanowire devices in biothreat applications. A test of selectivity was also carried out by characterizing the response of a

7

device to two different but structurally similar viruses, paramyxovirus and influenza A using nanowire devices modified with antibodies specific for influenza A. Delivery of a solution containing paramyxovirus exhibited only short duration conductance changes characteristic of diffusion of the virus past and/or rapid touching of the nanowire surface and not specific binding; however, when the solution was changed to one containing influenza A conductance changes consistent with well-defined binding/unbinding behavior similar to that in were observed.
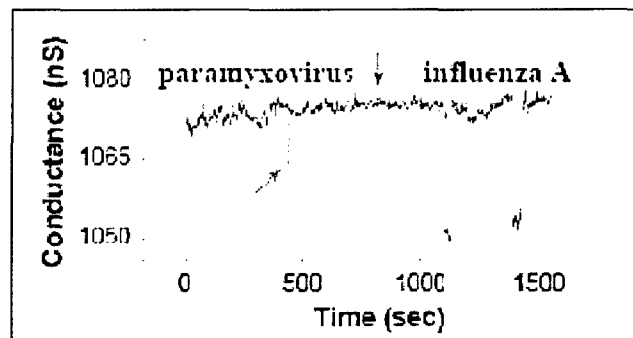
Importantly, these experiments demonstrate that the antibody-modified nanowire devices exhibit excellent binding selectivity, which is an important characteristic for detection of one or more viruses. While not our focus, these data also show that the devices are sensitive to single charged virus particles (including the sign of the charge) as they diffuse by and sample the nanowire surface, and this capability could find uses, for example, for charge detection in microfluidic devices.

3. Detection of in-field-like biosamples. The results described above demonstrate a unique level of sensitivity and selectivity, yet to impact in-field detection in the most significant way will require rapid analysis of relevant samples, such as blood serum. To this end we have also investigated the detection of PSA in undiluted donkey and human serum samples that were desalted by a rapid and simple purification step. The measurements were made using p-type silicon nanowire elements with either PSA Ab1 receptors (NW1) or surfaces passivated with ethanolamine (NW2) in the same sensor array. Conductance vs. time measurements recorded simultaneously from NW1 and NW2 as different donkey serum solutions were sequentially delivered to the devices are shown below. First, the introduction of donkey serum containing
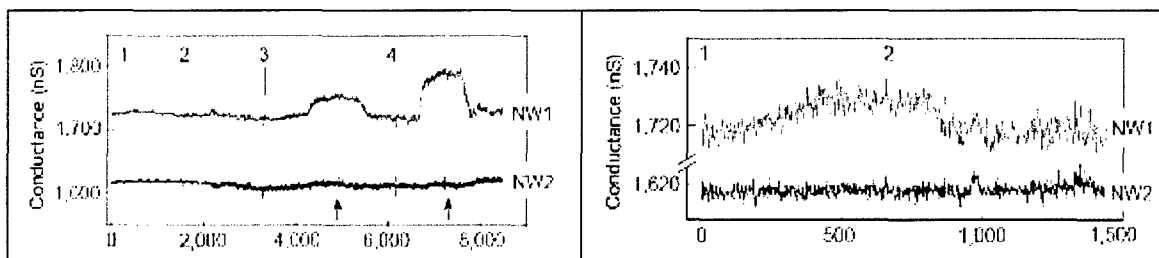

59 mg/ml total protein does not lead to appreciable conductance change relative to the standard assay buffer. Second, introduction of donkey serum solutions containing f-PSA led to concentration-dependent conductance increases only for NW1; no conductance changes were observed in NW2. Well-defined conductance changes were observed for PSA concentrations as low as 0.9 pg/ml, which corresponds to ~100 billion times lower concentration than that of the background serum proteins. Similar results were also obtained in conductance vs. time data recorded simultaneously from NW1 and NW2 for different

8

human serum samples. Specifically, addition of undiluted human serum, which contains f-PSA, blocked with an excess of Ab1 showed little change in baseline for either NW1 or NW2, although subsequent addition of undiluted human serum showed well-defined conductance increase in NW1. These results demonstrate clearly the ability to detect cancer markers with high sensitivity and selectivity in human serum.

4. Multiplexed detection of biological species: proteins, toxins & viruses. To test the capabilities of the nanowire arrays for multiplexed detection of proteins/toxins we first focused on prostate cancer where concentrations of both free PSA (f-PSA) and PSA-□1-antichymotrypsin (PSA-ACT) complex are generally measured. In our experiments, a device array was fabricated from p-type silicon nanowire elements that were then modified either with monoclonal antibody receptors for f-PSA, Ab1, or monoclonal antibody receptors that show cross-binding reactivity for f-PSA and the PSA-ACT complex, Ab2. Simultaneous conductance measurements of NW1, which was modified with Ab1, and NW2, which was modified with Ab2, were carried out for a wide-range of conditions. The data show that delivery of f-PSA resulted in concentration-dependent conductance changes in both NW1 and NW2, while the introduction of PSA-ACT yielded concentration-dependent conductance changes only in NW2. In addition, control experiments in which solutions of f-PSA, PSA-ACT, and Ab1 were delivered to the device array showed concentration conductance changes in NW2 but not NW1, since f-PSA was blocked by Ab1 present in the solution. These multiplexing results demonstrate selective, high-sensitivity detection of both markers, and show that nanowire sensor arrays could be used to measure the f-PSA and PSA-ACT concentrations in a single real-time assay.

More generally, multiplexed detection of distinct proteins, which will facilitate pattern analysis for robust threat identification, can be carried out with high sensitivity and selectivity using nanowire arrays modified with distinct antibody receptors as shown below. To test this
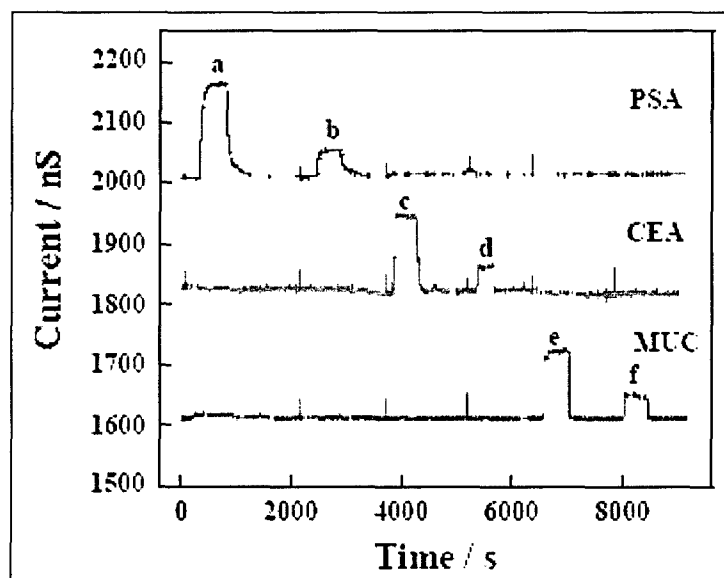
key capability we have investigated multiplexed detection of f-PSA, CEA, and Mucin-1 using silicon nanowire devices functionalized with monoclonal antibody receptors for f-PSA (NW1), CEA (NW2), and Mucin-1 (NW3). Conductance vs. time measurements were recorded simultaneously from NW1, NW2 and NW3 as different protein solutions were sequentially delivered to the device array as shown above. First, introduction of f-PSA and

9

buffer solutions led to concentration-dependent conductance increases only when NW1 was exposed to PSA solution; no conductance changes were observed in NW2 or NW3. Similarly, introduction of CEA solutions to the device array yielded concentration dependent conductance changes only in NW2, while subsequent delivery of mucin-1 solutions to the array resulted in concentration dependent conductance changes only in NW3. These results demonstrate the capability for multiplexed real-time, label-free marker protein detection with sensitivity to the femtomolar level and essentially complete selectivity.
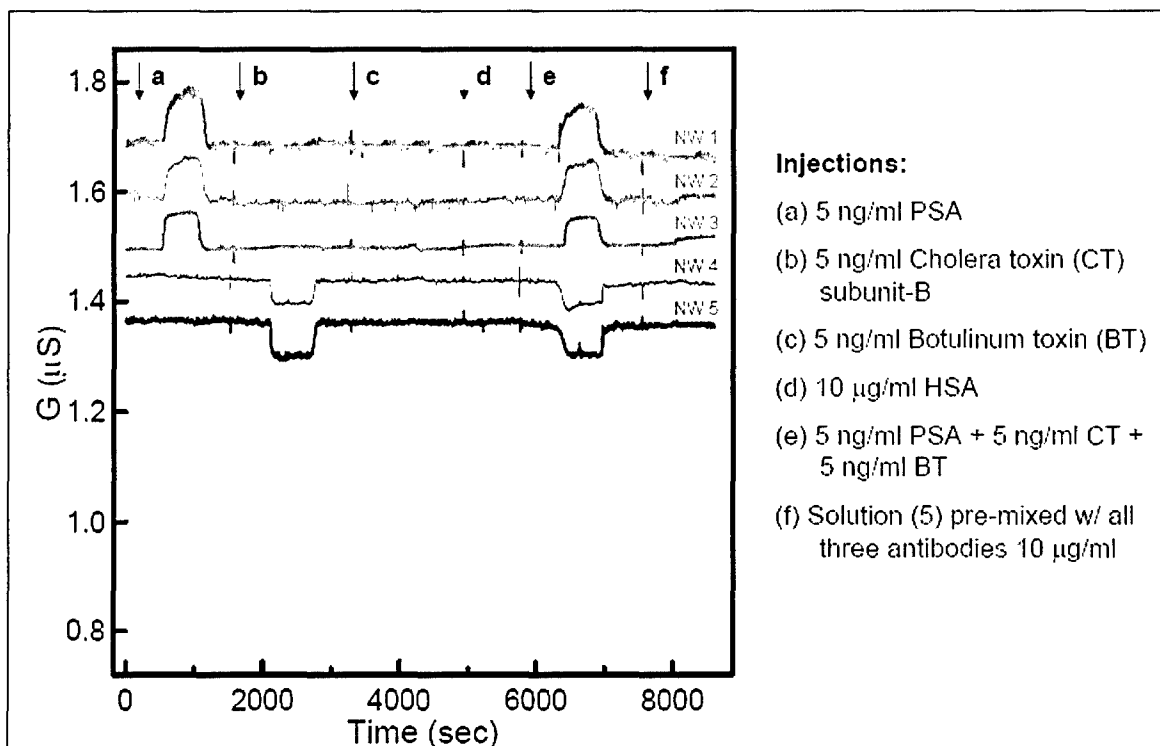
We also investigated multiplexed detection of different viruses at the single particle level by modifying nanowire device surfaces in an array with antibody receptors specific either for influenza A (NW-1) or for adenovirus (NW-2). Simultaneous conductance measurements obtained when adenovirus, influenza A, and a mixture of both viruses are delivered to the devices are shown below. Introduction of adenovirus, which is negatively charged at the pH of
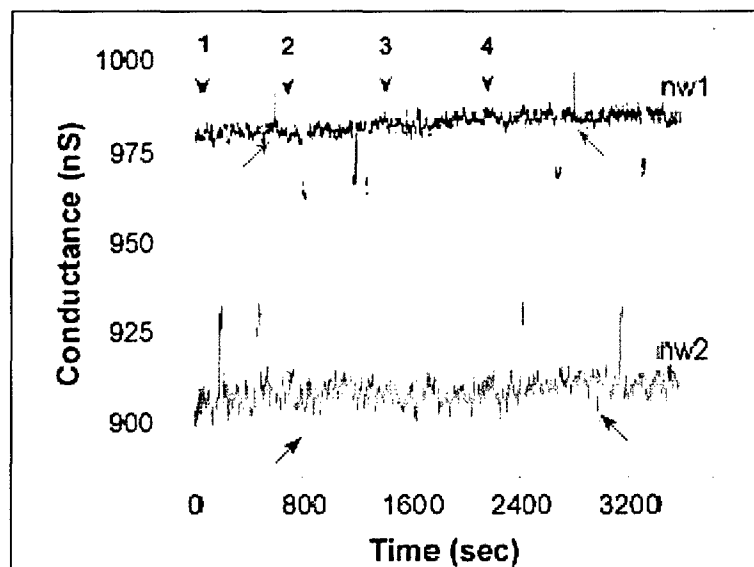
the experiment, to the device array yields positive conductance changes for nanowire-2 with an on time of 16 ± 6 s similar to the selective binding/unbinding for a comparable density of surface receptors. The magnitude of the conductance change for binding of single adenovirus particles differs from that of influenza A viruses due to differences in the surface charge densities for the two viruses. Shorter, ca. 0.4 s duration positive conductance changes are also observed for nanowire-1. These changes are characteristic of a charged virus diffusing past and rapidly sampling the nanowire element (see above) and can be readily distinguished from specific binding to the antibody receptors. On the other hand, addition of influenza A yields negative conductance changes for nanowire-1, with an binding/unbinding behavior similar to that observed in earlier experiments under comparable conditions. Nanowire-2 also exhibits short duration negative conductance changes, which likely correspond to diffusion of influenza A viral particles past the nanowire device, although these are also readily distinguished from specific binding events by the temporal response. Significantly, delivery of a mixture of both viruses demonstrates unambiguously that selective binding/unbinding responses for influenza A and adenovirus can be detected in parallel by nanowire-1 and nanowire-2, respectively, at the single virus level.

In addition, larger scale multiplexing was demonstrated with the simultaneous detection of multiple proteins and toxins using eleven p-type SiNW devices in a same array, named

10

NW1, NW2, ..., NW11. NW1-3 were modified with monoclonal antibody specific to prostate specific antigen (PSA), a cancer marker widely used for diagnosis of prostate cancer[28]; NW4-5 were modified with monoclonal antibody specific to cholera toxin subunit B (CTB); NW6-7 were modified with monoclonal antibody specific to botulinum toxoid type A (BTA); and NW8-11 were only incubated in the binding buffer without any antibodies. Time dependent conductance data recorded simultaneously from these nanowires is shown below.

Injections:

(a) 5 ng/ml PSA

(b) 5 ng/ml Cholera toxin (CT) subunit-B

(c) 5 ng/ml Botulinum toxin (BT)

(d) 10 μg/ml HSA

(e) 5 ng/ml PSA + 5 ng/ml CT + 5 ng/ml BT

(f) Solution (5) pre-mixed w/ all three antibodies 10 μg/ml

Delivery of 5 ng/ml of PSA solution (point a) led to an increase of conductance values of NW1-3, while the conductances of the other SiNW devices remained unchanged. Delivery of 5 ng/ml of CTB (point b) and BTA (point c) led to conductance decrease in the NW4-5 and conductance increase in NW 6-7, respectively, in good accord with the types of antibodies designated onto devices as well as the overall positive charge for CTB and overall negative charge for BTA. When a solution of human serum albumin (HSA) with much higher concentration (10 μg/ml) was delivered onto the device surface (point d), no significant conductance change was observed in all the eleven devices. Delivery of a mixed solution of PSA, CTB, and BTA, 5 ng/ml of each (point e), resulted in conductance changes on all the antibody-modified devices from NW1 to NW7, similar to the separate signals observed previously. Finally, when a mixed solution of three proteins (PSA, CTB and BTA, 5 ng/ml each) pre-incubated with excess of the respective free antibodies (10 μg/ml of all three antibodies) was delivered onto the device surface, the conductance values for all the eleven SiNW devices remained unchanged. This is expected since all the proteins had been blocked by the free antibodies before they could bind to the antibody receptors on the SiNW surface. These multiplexing results demonstrate the potential of using SiNW sensor arrays to parallel detect the binding/unbinding of a variety of proteins in a single label-free and real-time assay.

5. Ultrasensitive and multiplexed detection of chemical threats. The conversion of silicon nanowire field-effect transistors into ultrasensitive sensors for explosives detection was
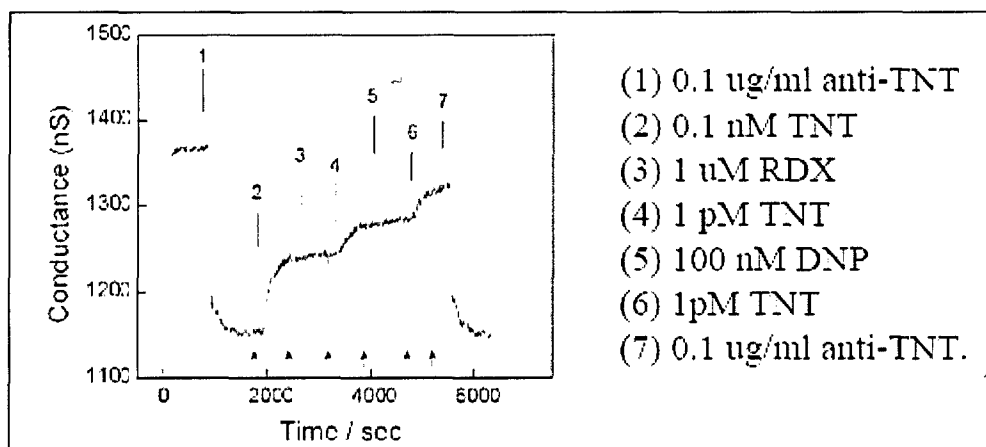
carried out by chemically modifying the nanowire surfaces following device fabrication. The basic linkage chemistry involves two key steps. First, aminopropyltrimethoxysilane (APTES) is coupled to oxygen plasma-cleaned silicon nanowire surfaces in order to present terminal amino groups at the nanowire surface. Second, the amino groups are coupled to the respective carboxyl-functionalized explosives analogs. Finally, the explosive-analogs modified nanoFET devices are incubated, using a microfluidic channel, with the respective anti-explosive antibodies, before the introduction of explosives samples during the displacement sensing step. The displacement of the charged antibody units from the nanowire surface, caused by the reaction with the small and uncharged free explosives molecules in sample, leads to changes in the electrical signal of the devices.

The sensitivity limits of the nanowire FET devices for explosives detection were first determined by measuring the conductance changes as the solution concentration of TNT was varied, where the devices were modified with the TNT-analog and preincubated, to saturation, with anti-TNT antibody (Fab fragments or whole antibody). Representative time-dependent simultaneous data from two nanowire-devices in the same array show a well-defined

(1) 0.1 ug/ml anti-TNT
(2) 1 nM TNT
(3) 0.1 ug/ml anti-TNT
(4) 1 nM TNT
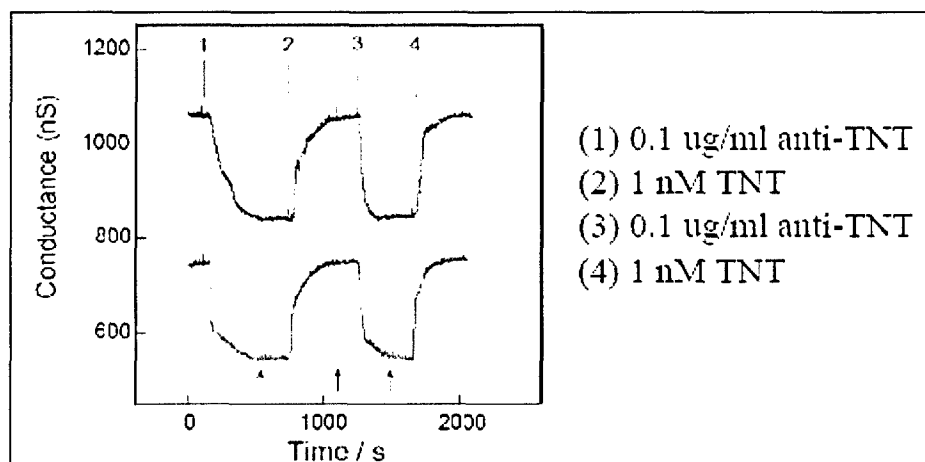
conductance decrease and the subsequent return to baseline when anti-TNT antibody (0.1 □g/ml) and TNT solutions (1 nM) respectively, are alternately delivered through a microfluidic channel to the TNT-analog modified devices.

The selectivity of the nanowire devices was investigated by cross-reactivity studies with various impurities and breakdown products of TNT, the explosives RDX and PETN, and other small molecules. Conductance versus time measurements recorded on a silicon nanowire device modified with TNT-analog **1** exhibited similar conductance changes is shown below.

12

(1) 0.1 ug/ml anti-TNT
(2) 0.1 nM TNT
(3) 1 uM RDX
(4) 1 pM TNT
(5) 100 nM DNP
(6) 1pM TNT
(7) 0.1 ug/ml anti-TNT.

When 0.1 nM and 1 pM solutions of TNT were delivered to the device. These results show that reproducible device to device sensitivity is achieved with these silicon nanowire sensors. Moreover, no conductance changes of the nanowire devices were detected after delivery of solutions containing 0.1 □M RDX or 100 nM DNP (dinitrophenol). These data demonstrate the excellent selectivity of the nanoFET devices in the detection of specific explosives.

To test the capabilities of the nanowire arrays for multiplexed detection of explosives, we first focused on the multiplexed detection of TNT, RDX, and PETN using silicon nanowire devices functionalized with the respective carboxy-functionalized explosive analogs, as depicted in below.
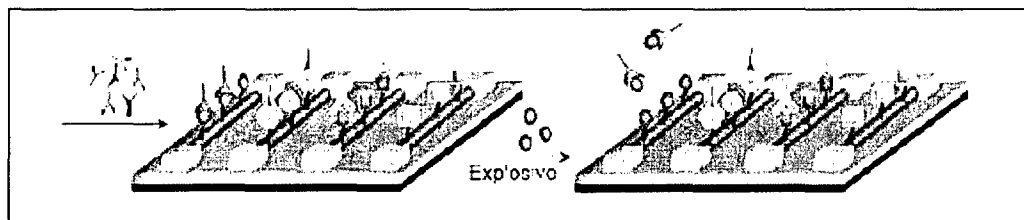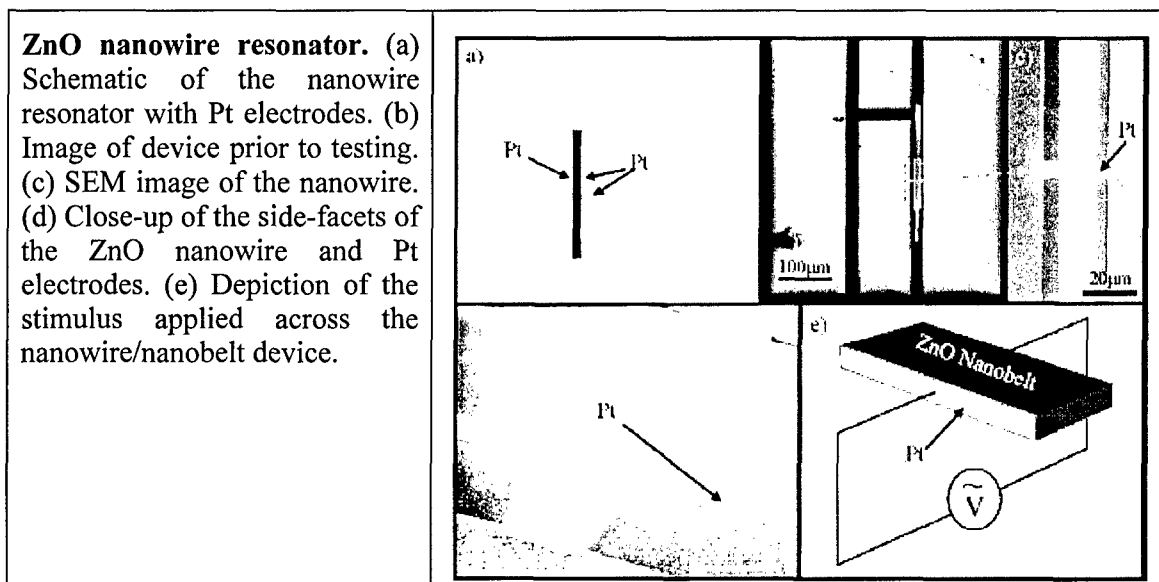

Conductance vs. time measurements were recorded simultaneously from NW1, NW2, NW3 and NW4 (control biotin-modified nanowire) as different explosive solutions were sequentially delivered to the device array preincubated with the respective explosive specific antibody. First, introduction of anti-TNT antibody, 0.1□gr/ml, and subsequent displacement

13
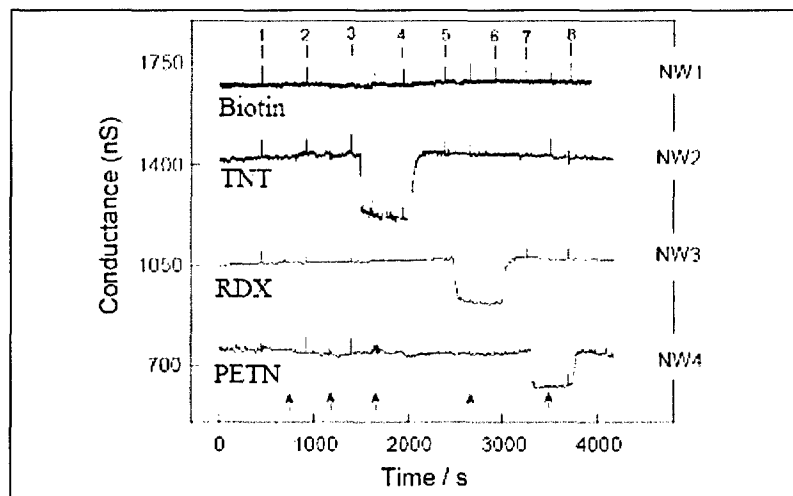
by TNT, 1 nM, sample solutions led to concentration-dependent conductance changes only on NW1 device; no conductance changes were observed in NW2, NW3 or NW4. Similarly, introduction of anti-RDX, 0.1□gr/ml, and RDX, 3 nM, solutions to the device array yielded conductance changes only in NW2, while subsequent delivery of anti-PETN, 0.1□gr/ml, and PETN, 5 nM, solutions to the array resulted in conductance changes only in NW3 (RDX and PETN antibodies shown not detected cross-reactivity with TNT-related compounds and between themselves). No conductance changes where detected on the biotin-modified NW4 used as an additional control to probe the specificity of the device array. These results demonstrate capability for multiplexed real-time, label-free explosives, and other small chemicals, detection with sensitivity down to the subpicomolar level and essentially complete selectivity.

6. Development of ZnO nanowire mass sensors. The bottom-up approach of nanotechnology has yielded many high quality, single crystal, and defect free structures like the nanobelt. Piezoelectric nanobelts of ZnO become attractive in these applications because of their perfectly faceted, beam-like geometry, making them ideal candidates as SMR, FBAR, and beam resonators. However, handling belts can be cumbersome when attempting to manipulate these materials into useful devices. In addition, the current operational frequency range for devices that utilize electro-mechanical filters are between 200 MHz and about 6 GHz. In order to fabricate devices that operate within this range, films on the order of 500 nm-15 μm thick are desired.

Under the support of DARPA, a bulk acoustic resonator based on ZnO belts was demonstrated. This device shows a great deal of promise in applications as an electronic

ZnO nanowire resonator. (a) Schematic of the nanowire resonator with Pt electrodes. (b) Image of device prior to testing. (c) SEM image of the nanowire. (d) Close-up of the side-facets of the ZnO nanowire and Pt electrodes. (e) Depiction of the stimulus applied across the nanowire/nanobelt device.


filter, as well as a mass sensor. The fabricated device was characterized using vector network analysis and both the first and third harmonics of resonance were observed at approximately 247MHz and 754MHz, respectively. An one-dimensional Krimholt-Leedom-Matthaei model was utilized to predict the resonant frequency of the device and confirm the observed behavior.

14

7. Development of unique signal analysis methods. Given the output of a multiplexed array with nanowires modified with a known set of modifiers, what is the content of the analyzed sample? Variants of this include: Is a given virus present, and what is the most likely mix of viruses. Given a desired list of viral agents of interest, what is an effective approach to selecting modifiers so as to detect and distinguish the agents of interest? Factors to consider include achieving adequate redundancy to tolerate nanowire failures as well as a selection of modifiers that covers the space of viral agents of interest.

Our approaches are based on the representation of the array response to a viral agent as a pattern of conductance change over nanowires with known modifiers. This representation permits analysis of the output of such an array via belief network (Bayes) methods, as well as combinatorial methods such as linear programming. Our development explicitly comprehends "noisy" output from the array, caused by either faulty nanowires or contaminants. A nanowire modified with specific antibody receptors responds to viral bindings as follows. Viral particles sampling but not binding to a receptor site on the wire cause a transient change in conductance, which manifests as a spike of brief duration in a trace of conductance versus time. Transient spikes are also observed coincident with fluidic injections, and these spikes may correlate across nanowires in a multiplexed array so as to allow removal of noise features correlated across wires. Specific bindings appear as a "boxcar" change in conductance, either positive or negative, depending on solution pH and the charge of the modifier. For a given concentration, the duration of the boxcar in time is fairly consistent, as is the amplitude change. The observed response corresponds to single viral particle bindings, and the interval of conductance change corresponds to a particle attaching, remaining bound for some time interval, and then releasing, as confirmed by electron micrograph. Some cases of multiple bindings to the same wire have been observed by the Harvard team; these appear as superimposed boxcars in the trace.

An idealized conductance trace for a single nanowire, showing a transient spike feature corresponding to a non-specific contact, a boxcar corresponding to a specific binding, and a superimposed boxcar corresponding to a specific binding followed by a second specific binding before the first particle releases.

Idealized conductance trace showing, respectively, non-specific transient spike, specific binding, and superimposed specific bindings	
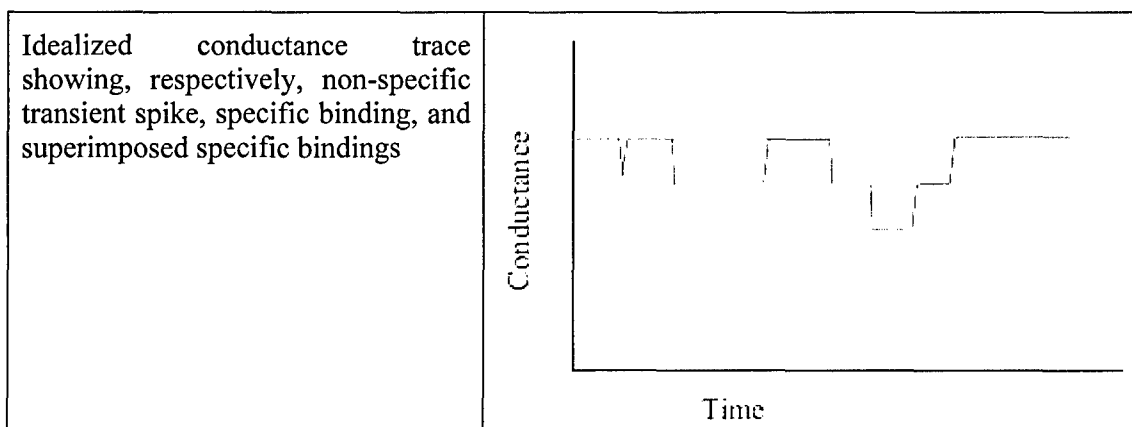
An actual trace of data from the Lieber is shown below. There are two nanowires, the first modified with anti-Influenza Type A antibody (NW1) and the second with anti-adenovirus group III (NW2). The noise characteristics and boxcar shapes are typical of what we have observed, although these traces do not exhibit significant trends.

15
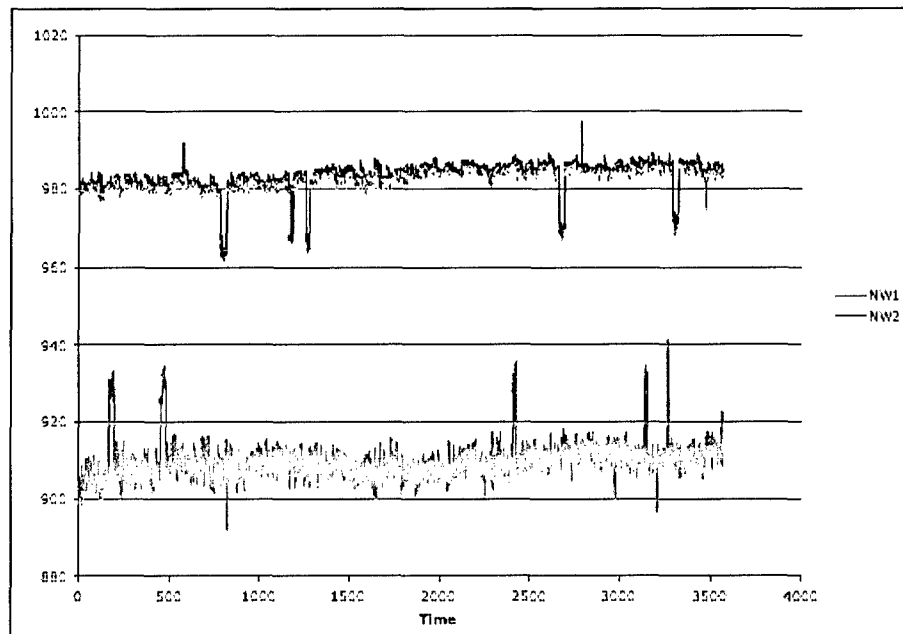
Matched filtering describes a variety of techniques whereby a representation of a signal of interest is convolved with a series or image in which the signal may or may not be present. Regions that agree well with the matched filter will correspond to local maxima in the matched filter output. These local maxima are declared to be instances of the signal of interest if they are above some threshold.

For reasons of computational efficiency, both signal and data are transformed, typically using a Fast Fourier Transform (FFT). Convolution corresponds to point wise multiplication in transform space.

Matched filtering is an optimal detection algorithm in the case of additive signal in white noise. Much of the efficacy in the approach depends on conditioning of the data so as to satisfy this assumption. Common noise sources include:

- Uncorrelated noise, which is often effectively removed by subtracting the data mean and dividing by the standard deviation.

- Frequency content (in time or space), removed by estimation of and then dividing out the power spectrum.

- Trends, which must be estimated and removed.

- Signal capture, in which the signal is sufficiently strong so as to significantly influence estimates of noise, frequency content, or trend. For example, in typical conductance traces in our case, the magnitude and duration of amplitude changes due to specific bindings are sufficient to affect sample statistics.

For simplicity, our initial matched filter analysis considered only uncorrelated noise. As such, the data normalization procedure is simply to subtract the grand mean and divide by the standard deviation. This simple procedure achieves a degree of data whitening.

A matched filter is an idealization of the hypothesized signal one is trying to detect in the data. In this case, the matched filter is a manually constructed -20 nS boxcar of duration 20 s. For FFT indexing reasons, this is "unwrapped" to comprise 10 points of value -20 in the first 10 positions and 10 points of value -20 in the last 10 positions of an array 1024 long, which is

16

otherwise zero. The matched filter is approximately whitened by dividing by the standard deviation of the conductance data. We focused on the interval from 500 to 1523 seconds, which provides 1024 points and is a convenient array size for Fourier analysis. Over this interval, NW1 exhibits spike features only, so we focus on NW2 which exhibits one spike and three boxcars. The whitened data and matched filter are processed through a Fast Fourier Transform (FFT). The convolution of the matched filter and the data is achieved in transform space as elementwise multiplication of the Fourier series. An inverse transform produces the matched filter output, which is then normalized by dividing by its own standard deviation (it is in theory zero mean – the mean we obtained here was 1.8e-11). The data below shows the normalized data trace for wire 2 as well as the matched filter output.
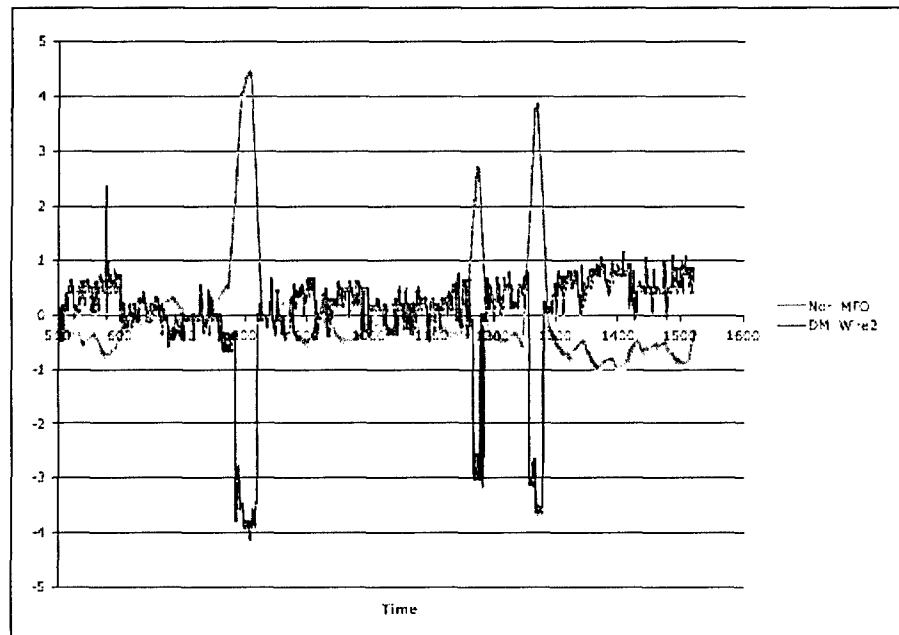
Peaks in the matched filter output correspond to regions of maximal match between the data and the filter. Although this is a somewhat simple case, we observe as expected three matched filter peaks corresponding to the bindings of interest, with no matched filter ringing at the transient spike or anywhere else along the trace.

Histogram Detrending and Advanced Detection. Data below shows a nanowire modified for Influenza detection, in an experiment where first Influenza only and then a mixture of Influenza and Parmyoxovirus are introduced. The latter introduction is immediately before the break in the trend (at time 1300).

17
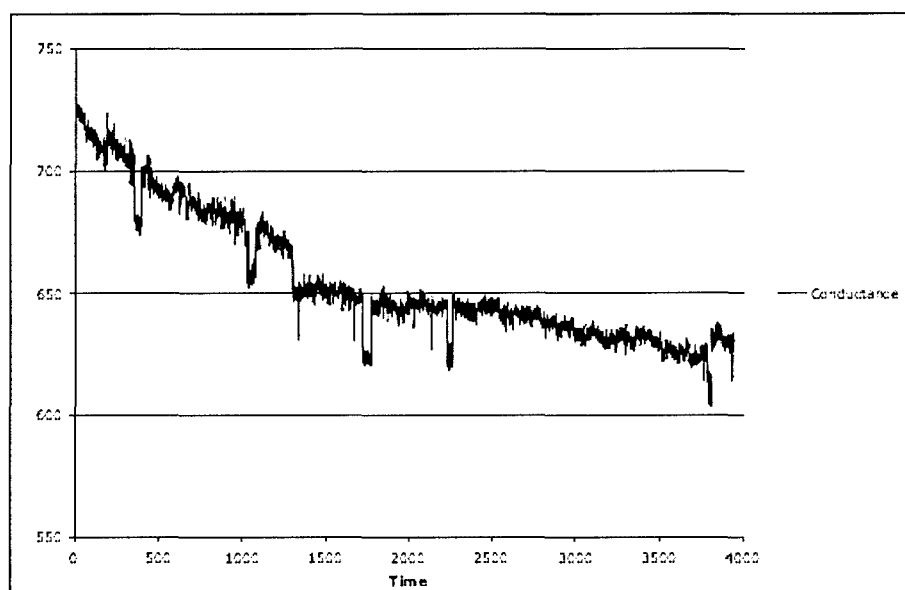
This influenza/parmyoxovirus data show a significant nonlinear trend and also contains signal transitions that deviate from the boxcar model (possibly the result of sequential virus binding/unbinding). Data such as this requires more sophisticated processing than presented above in order to estimate and remove the trend. Three detrending approaches were tried with this data. The first method is a conventional curve fitting method in which we fit a global function to the entire data set and subtract that function from the data (assuming that the fitted function represents the data trend). The global fitting approach turned out to be undesirable because the change in conductance at approximately 1300 seconds produces a persistent shift in the data mean and biases the trend locally. Another approach is to model the trend locally using a moving average. The trend and bias removal is better than for the previous fitted trend removal case. However, the moving average still shows some variation near binding events. Nonetheless, this result is much more appropriate for other modeling (e.g. autoregression) and detection techniques (matched filtering).

Finally, a more sophisticated approach is taken in which a histogram is utilized to obtain a more accurate representation of the local mean. In this approach, a histogram is computed in much the same way as the moving average. In this case, histograms are successively computed over a 200 second moving window. Each histogram represents a density function of the conductance values within the window. Since the data is largely characterized by slowly moving trends and boxcar or step functions, the histograms will typically exhibit one or two distinct populations, the latter in the case that the window contains significant points from the background and the signal.

By using the maximum value of the largest population in the histogram, we can estimate the mean value of the local window in the data. Step changes in the data will be regarded as sudden changes in the mean as opposed to a bind or unbind signature unless additional measures are taken. We process the original data by choosing the value of conductance for the maximum count value of each histogram as the local mean at that point. Then we move the window and repeat the computation for each point in the original time series. The original time series data detrended by this model is shown below.

18

Detrended Conductance (nS)
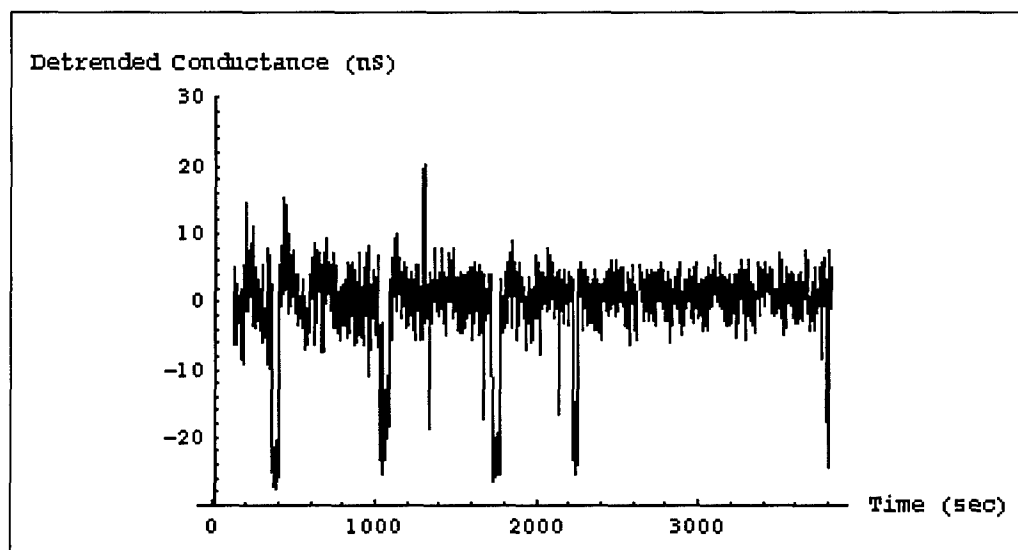
With the histogram model, the bias and trend removal is more stable near binding events. From a qualitative point of view, the signal to noise ratio seems slightly greater with the histogram model. One disadvantage with this method is that the single step in the data at 1300 seconds appears as a spike rather than as a boxcar function – additional analysis might be necessary to detect these transitions if that were desirable. Another disadvantage of this method is that it is computationally much more expensive than the others. However, this method can be applied incrementally as data is gathered, so the cost may not be significant.

Detection in notional multiplexed nanowire arrays. Our team has proposed multiplexed arrays for more reliable detection of viral agents (reliability achieved through redundant nanowires similarly modified) as well as detection of diverse agents with a single array. To date, the team has built arrays with fewer than ten wires and limited redundancy. The eventual objective is to scale to arrays of hundreds or thousands of nanowires. Multiplexed arrays will consist of multiple nanowires modified with the same antibody, drawn from an antibody library. Ideally an antibody is specific to a viral agent. In practice, we expect to see some weak bindings (lower amplitude conductance change and/or shorter duration of binding) in the case of an antibody specific to a virus variant from the same family as the viral agent being analyzed in a given run. For example, an adenovirus variant is expected to exhibit strong bindings to wires modified with antibodies specific to the variant, and weaker binding to some wires modified with antibodies specific to other adenovirus variants. Bindings to wires modified for other viral families (for example, adenovirus bindings to wires modified with influenza antibodies) are expected to be rare.

A simple detection approach that might prove robust for many types of nanowire data is simple threshold testing. In testing for substantial viral or chemical concentrations (as opposed to single virus or particle detection), one can expect binding-event signals such as in the above figure lasting 10s to 100s of seconds as compared to noise events (~1 second). In such a case, low pass filtering can remove a large percentage of electrical noise and spiky "sampling" events on the nanowires. The resulting signal can be tested against a threshold to detect the presence of a binding event.

As an example, we use the CT antibody nanowires NW1 and NW2 from data provided by Lieber. Applying a low-pass filter to the NW1 and NW2 data result in the signatures shown below. Applying a threshold on the negative-going waveform produces detections of the

19

NW1 CT

NW2 CT

Seconds
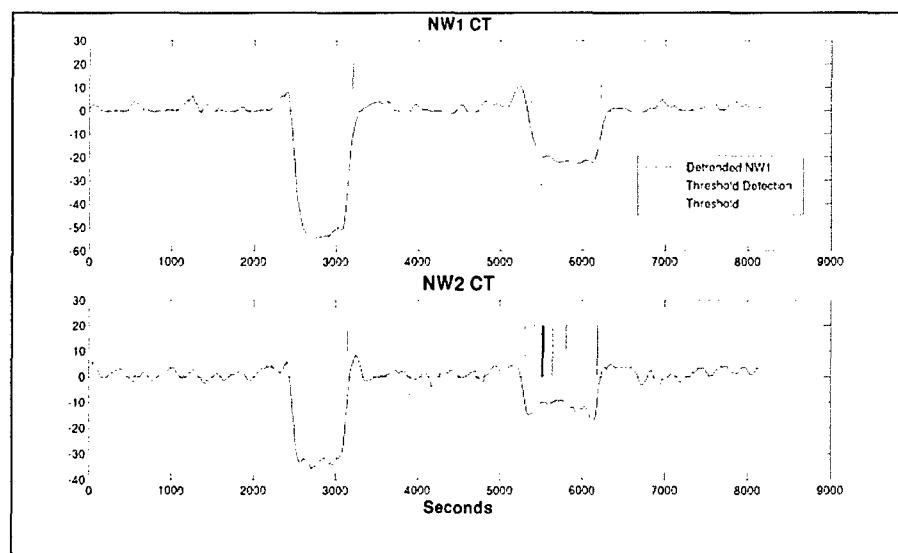
binding events. The result from NW2 demonstrates that care must be taken in setting the threshold. One trades detection sensitivity against the likelihood of false alarms in noisy data. If the threshold is set too close to the origin, the algorithm will interpret excursions in the noise as detections. A threshold too far away from the origin will miss lower amplitude conductance changes due to lower concentration samples.

The appropriate filtering and threshold value depends on the requirements for the particular application. A separate threshold would likely be necessary for each wire in an array - awkward for very large arrays. However, the threshold could be adaptively set depending on the background noise. A one-time calibration phase where the instrument is run on a neutral sample (to determine noise levels) or subjected to actual samples would allow calibration of the algorithm. It would also be possible to dynamically adjust thresholds (and thus false alarm rate or sensitivity) while the instrument runs by maintaining some instantaneous measure of background noise for each nanowire. At the very least, individual thresholds would be necessary to accommodate junction variations from the fabrication process. An advantage of the threshold technique is that it is simple and very well understood. It is also very easy to pass event width and height information along for more processing – for instance, determining the concentration of a virus as well as its presence or combining the signature of several similarly treated nanowires. A disadvantage to the threshold approach is susceptibility to noise. The matched filter or correlation filter techniques are much more resistant to non-Gaussian noise because they would depend on the overall "boxcar" shape of the signature. However, the width and height of binding signatures can change depending on solution concentration and pH. The matched filter approach would require a bank of matched filters for various "boxcar" dimensions or some normalization calculation to map the signatures to a standard width or height.

The preceding results mostly agree with intuition, but with some exceptions. The noise models underlying the situation are ad hoc, but we observe ambiguity in the case of competing bindings or non-specific bindings. It is essential to characterize the noise in the response from multiplexed arrays. This noise will be reduced as similarly modified nanowires are replicated in greater numbers. However, we should not assume the noise reduction that would be obtained from independent replicates because the wires may respond similarly for some underlying common mode effect (for example, a process artifact for a batch of wires similarly modified).

20

C. PUBLICATIONS STEMMING FROM RESEARCH EFFORT

C. M. Lieber, Harvard University

1. J. Hahm and C.M. Lieber, "Direct Ultrasensitive Electrical Detection of DNA and DNA Sequence Variations Using Nanowire Nanosensors," *Nano Lett.* **4**, 51-54 (2004).

2. Y. Wu, Y. Cui, L. Huynh, C.J. Barrelet, D.C. Bell and C.M. Lieber, "Controlled Growth and Structures of Molecular-Scale Silicon Nanowires," *Nano Lett.* **4**, 433-436 (2004).

3. S. Jin, D. Whang, M.C. McAlpine, R.S. Friedman, Y. Wu and C.M. Lieber, "Scalable Interconnection and Integration of Nanowire Devices without Registration," *Nano Lett.* **4**, 915-919 (2004).

4. L.J. Lauhon, M.S. Gudiksen and C.M. Lieber, "Semiconductor nanowire heterostructures," *Phil. Trans. R. Soc. Lond. A* **362**, 1247-1260 (2004).

5. Y. Wu, J. Xiang, C. Yang, W. Lu and C.M. Lieber, "Single-crystal metallic nanowires and metal/semiconductor nanowire heterostructures," *Nature* **430**, 61-65 (2004).

6. D. Whang, S. Jin and C.M. Lieber, "Large-Scale Hierarchical Organization of Nanowires for Functional Nanosystems," *Japanese J. Appl. Phys.* **43**, 4465-4470 (2004).

7. D.C. Bell, Y. Wu, C.J. Barrelet, S. Gradecak, J. Xiang, B.P. Timko and C.M. Lieber, "Imaging and Analysis of Nanowires," *Microsc. Res. Tech.* **64**, 373-389 (2004).

8. F. Patolsky, G. Zheng, O. Hayden, M. Lakadamyali, X. Zhuang and C.M. Lieber, "Electrical detection of single viruses," *Proc. Natl. Acad. Sci. USA* **101**, 14017-14022 (2004).

9. G. Zheng, W. Lu, S. Jin and C.M. Lieber, "Synthesis and Fabrication of High-Performance n-Type Silicon Nanowire Transistors," *Adv. Mater.* **16**, 1890-1893 (2004).

10. Y. Huang and C.M. Lieber, "Integrated nanoscale electronics and optoelectronics: Exploring nanoscale science and technology through semiconductor nanowires," *Pure Appl. Chem.* **76**, 2051-2068 (2004).

11. W.U. Wang, C. Chen, K. Lin, Y. Fang and C.M. Lieber, "Label-free detection of small-molecule-protein interactions by using nanowire nanosensors," *Proc. Natl. Acad. Sci. USA* **102**, 3208-3212 (2005).

12. F. Patolsky and C.M. Lieber, "Nanowire nanosensors," *Materials Today* **8**, 20-28 (2005).

13. Y. Huang, X. Duan and C.M. Lieber, "Semiconductor Nanowires: Nanoscale Electronics and Optoelectronics," in *Dekker Encyclopedia of Nanoscience and Nanotechnology*, J.A. Schwarz, Ed. (Marcel Dekker, Inc., 2005).

14. X. Duan and C.M. Lieber, "Semiconductor Nanowires: Rational Synthesis," in *Dekker Encyclopedia of Nanoscience and Nanotechnology*, J.A. Schwarz, Ed. (Marcel Dekker, Inc., 2005).

15. Z. Zhong, Y. Fang, W. Lu and C.M. Lieber, "Coherent Single Charge Transport in Molecular-Scale Silicon Nanowires," *Nano Lett.* **5**, 1143-1146 (2005).

16. G. Zheng, F. Patolsky, Y. Cui, W.U. Wang and C.M. Lieber, "Multiplexed electrical detection of cancer markers with nanowire sensor arrays," *Nat. Biotechnol.* **23**, 1294-1301 (2005).

17. C. Yang, Z. Zhong and C.M. Lieber, "Encoding Electronic Properties by Synthesis of Axial Modulation Doped Silicon Nanowires," *Science* **310**, 1304-1307 (2005).

18. F. Patolsky, G. Zheng and C.M. Lieber, "Nanowire-based biosensors," *Anal. Chem.,* in press.

19. F. Patolsky, G. Zheng and C.M. Lieber, "Nanowire Sensors for Medicine and the Life Sciences," *Nanomedicine.,* in press.

X. Zhuang, Harvard University

1. M. Lakadamyali, M. J. Rust, X. Zhuang, "Ligands for clathrin-mediated endocytosis are differentially sorted into distinct populations of early endosomes," *Cell* **124,** 997-1009 (2006)

2. Y. Zhou, X. Zhuang, "Robust reconstruction of the probability distributions of kinetic rate constants", *submitted for publication.*

3. J. Zheng, X. Zhuang, "Silver superclusters: a ultrabright silver nanostructure for fluorescence imaging and Raman sensing", *in preparation.*

Z. L. Wang, Georgia Institute of Technology

1. Brent A. Buchine, William L. Hughes, F. Levent Degertekin, Zhong L. Wang[*] "Bulk Acoustic Resonator Based on Piezoelectric ZnO Belts", Nano Letters, published online (2006).

2. Zhong Lin Wang* and Jinhui Song "Piezoelectric Nanogenerators Based on Zinc Oxide Nanowire Arrays", Science, 312 (2006) 242-246.

3. Xudong Wang, Jinhui Song, Christopher J. Summers, Jae Hyun Ryou, Peng Li, Russell D. Dupuis, and Zhong L. Wang* "Density-Controlled Growth of Aligned ZnO Nanowires Sharing a Common Contact - A simple, low-cost and mask-free technique for large-scale applications", J. Phys. Chem. B, 110 (2006) 7720-7724.

D. PRESENTATION OF RESEARCH STEMMING FROM RESEARCH EFFORT

C. M. Lieber, Harvard University, Invited Talks

1. 5 May 2005 - Samuel McElvain Seminar Series (Materials Chemistry Division), University of Wiconsin-Madison
"Nanoscience and the Pathway to Nanotechnologies"

2. 16 May 2005 – Gerhard Schmidt Memorial Lecture, Weizmann Institute of Science, Israel
"Nanoscience & Nanotechnology: Emerging Opportunities in Electronics, Biology and Much More!"

3. 7 June 2005 – International Symposium on "Chemistry in the Emerging Fields of Nanotechnology and Biotechnology," Seoul National University, South Korea
"Nanotechnology: From Fundamental Science to Emerging Opportunities in Electronics, Biology and Much More!"

4. 8 June 2005 – Samsung SAIT, South Korea
"Nanotechnology: From Fundamental Science to Emerging Opportunities in Electronics, Biology and Much More!"

5. 9 June 2005 – China NANO 2005, Beijing China
Plenary: "Nanotechnology: Emerging Opportunities in Electronics, Biology and Much More!"

6. 9 June 2005 – Molecular Science Forum, Chinese Academy of Sciences, China
"Nanowires for Nanoscience and Nanotechnology"

7. 21 June 2005 – 65th Annual Physical Electronics Conference, University of Wisconsin-Madison
Keynote: "Nanoscience and the Pathway to Nanotechnologies"

8. 7 September 2005 – Second Focused Workshop on Electronic Recognition of Bio-molecules, University of Illinois at Urbana-Champaign
Plenary: "From Ultrasensitive Detection to Active Interfaces with Biological Systems Using Nanowire Nanoelectronics"

9. 29 September 2005 – MESA+ Day Annual Meeting 2005, University of Twente, The Netherlands
Plenary: "Nanowires for Nanoscience and Nanotechnology"

10. 6 October 2005 – Symposium on Semiconductor Nanowires, Lund University, Sweden
Keynote: "Nanowires, Nanoscience and Emerging Nanotechnologies"

11. 24 October 2005 – Optics East 2005, Boston MA
Keynote: "Nanowire based electrical sensors for multiplexed detection of biological/chemical species down to single particle level, and new advances in

23

nanophotonic sources/detectors for integrated optical-based sensing and/or photon detection"

12. 7 November 2005 – Fifth Annual Richard M. and Patricia H. Noyes Lectureship, University of Oregon
    "Science and Technology at the Nanoscale"

13. 8 December 2005 – International Semiconductor Device Research Symposium 2005, Bethesda MD
    Plenary: "Nanowires for Nanoscience and Nanotechnology"

14. 28 February 2006 – Gordon Research Conference on Bioanalytical Sensors, Ventura CA
    "Nanowire Nanosensors"

15. 2 March 2006 – Applied Biosystems meeting, Foster City CA
    "Nanowire Device Arrays for Multiplexed Detection, Kinetics and Cellular Assays"

16. 4 April 2006 – MITRE Workshop on Nanosensors for Nose-Like Sensing, McLean VA
    Keynote: "Toward Nanowire Bio-sensing Systems"

17. 25 April 2006 – Samsung Semiconductor Technology Advisory Committee Forum 2006, Seoul Korea
    "Nanowires and the Pathway to Multi-Functional Integrated Systems"

18. 26 April 2006 – Peking University College of Engineering Distinguished Lecture, Beijing China
    "Nanowires and Pathways to Nanotechnologies"

C. M. Lieber Group, Harvard University

19. 29 August 2005 – ACS Fall 2005 Meeting, Washington DC
    "Large-scale, multiplexed electrical detection of proteins and viruses by ultrasensitive nanowire sensor arrays"
    (Gengfeng Zheng – Invited Talk)

20. 29 November 2005 – MRS Fall 2005 Meeting, Boston, MA
    "Single-crystal Silicon Nanotubes, Hollow Nanocones, and Branched Nanotube Networks"
    (Brian Timko – Contributed Talk)

21. 29 November 2005 – MRS Fall 2005 Meeting, Boston, MA
    "Metal-Semiconductor Nanowire Heterostructures"
    (Yue Wu – Contributed Talk)

22. 30 November 2005 – MRS Fall 2005 Meeting, Boston, MA
    "Large-scale, Label-free, Parallel Electrical Detection of Proteins, Nucleic Acids and Viruses by High-throughput Ultrasensitive Nanowire FET Arrays"

(Gengfeng Zheng – Contributed Talk)

23. 17 March 2006 – 2006 APS March Meeting, Baltimore, MD
"Challenges and Issues in Nanowire Nanodevices"
(Robin Friedman – Invited Talk)

24. 26 March 2006 – 231st ACS National Meeting, Atlanta, GA
"General and Powerful Platform for Large-scale, Label-free Parallel Electrical Detection of Biomolecules by Ultrasensitive Nanowire Transistor Arrays"
(Gengfeng Zheng – Contributed Talk)

25. 19 April 2006 – 2006 MRS Spring Meeting, San Francisco, CA
"General and Powerful Platform for Large-scale, Label-free, Parallel Electrical Detection of Biomolecules by Ultrasensitive Nanowire Transistor Arrays"
(Gengfeng Zheng – Contributed Talk)

26. 19 April 2006 – 2006 MRS Spring Meeting, San Francisco, CA
"Electronic Interface Between Nanowires and Neurons"
(Brian Timko – Poster Presentation)

27. 9 May 2006 – 2006 NSTI Nanotechnology and Trade Show, Boston, MA
"Early Cancer Detection Using Silicon Nanowires Electrical Devices"
(Fernando Patolsky – Invited Talk)

X. Zhuang, Harvard University

1. Gordon Research Conference on Lysosomes and Endocytosis (2006)

2. Gordon Research Conference on Single Molecule Approach to Biology (2006)

3. University of Michigan International Symposium on "At the Single Molecule Frontier: Integration in Biology and Nanotechnology" (2006)

4. Royal Society of Chemistry Symposium on Frontiers in Chemical Biology, England (2006)

5. Annual Meeting of the Biophysical Society, 50th anniversary symposium speaker (2006)

6. American Chemical Society National Meeting (2006)

7. American Chemical Society National Meeting (2005)

8. International Congress in Biophysics, France (2005)

9. Annual Meeting of the Biophysical Society (2005)

10. Biophysics Seminar, Columbia University (2006)

11. BCMP Seminar, Harvard Medical School (2006)

12. Molecular and Medical Pharmacology Seminar, UCLA (2006)

13. Annual Life Sciences Symposium, Dartmouth College (2006)

14. Department of Chemistry, Ohio State University (2006)

15. Department of Chemistry, Stanford University (2005)

16. School of Chemistry and Biochemistry, Georgia Institute of Technology (2005)

17. Biochemistry/Molecular Biophysics seminar, JILA (2005)

18. Department of Chemistry, Brandeis University (2005)

19. Department of Applied Physics, California Institute of Technology (2005)

20. Biophysics/Chemical Biology Seminar, UCSF (2005)

21. Department of Physics, University of California at Berkeley (2005)

22. Department of Chemistry, Massachusetts Institute of Technology (2005)

23. Department of Biomedical Engineering, University of Texas at Austin (2005)

24. Department of Chemistry, Rutgers University (2005)

25. Department of Chemistry, University of Pennsylvania (2005)

26. Department of Chemistry, Columbia University (2005)

Z. L. Wang, Georgia Institute of Technology

1. "Polar-surface induced novel growth configurations of piezoelectric nanobelts", Invited talk in SPIE, Boston, Oct. 23-27, 2005.

2. "ZnO – the nanomaterial after carbon nanotubes", in Advisory Board Meeting, Institute of Semiconductor, CAS, Beijing, China, Oct. 17-18, 2005.

3. "Helixing of oxide nanobelt", invited lecture at Universie Pierre et Marie Curie, France, Oct. 13, 2005.

4. "From nanocrystals to nanowires", invited lecture at Universie Pierre et Marie Curie, France, Oct. 14, 2005.

5. "Polar surface dominated novel nanostructures of ZnO", invited lecture in a Symposium in Honor of Prof. Z.L. Wang Universie Pierre et Marie Curie, France, Oct. 12, 2005.,

6. "Semiconducting and piezoelectric nanostructures of ZnO – the material after carbon nanotubes", seminar series in nanotechnology, GE Research Center, Albany, NY, Sept. 27, 2005.

7. "Discovering and understanding the growth of novel nanostructures by electron microscopy" (Plenary), EMAG-Nano 2005, Institute of Physics (UK), University Leeds, UK, Aug. 31-Sept. 2, 2005.

8. "Nanostructures and nanodevices of oxide nanobelts", Dept. of Physics, University of Birmingham, UK, Sept. 2, 2005.

9. "Heix and helixing of ZnO nanobelt", University of Science and Technology of China, Hefei, China, Aug. 9, 2005.

10. "Nanostructures of ZnO" (keynote), International Conference on Materials for Advanced Technologies (ICMAT2005), Singapore, July 3-7, 2005.

11. "Discovery of oxide nanobelts" (T.D. Lee Lecture), Graduate School of Chinese Academy of Science, Beijing, June 30, 2005.

12. "Nanostructures of ZnO – a material after carbon nanotube", Annual meeting on Electronic Materials, TMS, Santa Barbara, June 22-24, 2005.

13. "Materials chemistry and physics of one-dimensional oxide nanostructures", Fudan University, May 26, 2005.

14. "Materials and devices of oxide nanobelts", The 15th Lecture on Semiconductor Electronics, The Institute of Semiconductors, Beijing, May 25, 2005.

15. "One-dimensional oxide nanostructures", The 1st China-US Workshop on Materials Science, Beijing, May 23-25, 2005.

16. "Updated progress in oxide nanostructure research", invited lecture at Universie Pierre et Marie Curie, France, May 10, 2005.

17. "Novel piezoelectric devices based on nanobelts", invited lecture at Universie Pierre et Marie Curie, France, May 12, 2005.